REVIEW OF SCIENTIFIC INSTRUMENTS **87**, 045103 (2016)

# Apparatus for low temperature thermal desorption spectroscopy of portable samples

S. Stuckenholz, C. Büchner, H. Ronneburg,[a] G. Thielsch, M. Heyde,[b] and H.-J. Freund
*Fritz-Haber-Institut der Max-Planck-Gesellschaft, Faradayweg 4-6, 14195 Berlin, Germany*

(Received 9 October 2015; accepted 19 March 2016; published online 5 April 2016)

An experimental setup for low temperature thermal desorption spectroscopy (TDS) integrated in an ultrahigh vacuum-chamber housing a high-end scanning probe microscope for comprehensive multi-tool surface science analysis is described. This setup enables the characterization with TDS at low temperatures (T > 22 K) of portable sample designs, as is the case for scanning probe optimized setups or high-throughput experiments. This combination of techniques allows a direct correlation between surface morphology, local spectroscopy, and reactivity of model catalysts. The performance of the multi-tool setup is illustrated by measurements of a model catalyst. TDS of CO from Mo(001) and from Mo(001) supported MgO thin films were carried out and combined with scanning tunneling microscopy measurements. © *2016 AIP Publishing LLC.* [http://dx.doi.org/10.1063/1.4945265]

## I. INTRODUCTION

Surface science studies are important to understand reaction mechanisms on a fundamental level.[1] Since every surface science method has its limitations in terms of information, the ideal setup offers several high-end techniques that can be applied to the same sample surface.

Unfortunately, each technique places different requirements on the sample setup. Thermal desorption spectroscopy (TDS) is used for studying surface kinetics and desorption energies, and has been a widely applied technique for decades.[2–4] With the support of theoretical models, desorption peaks can be assigned to specific adsorption sites.[5,6] In setups performing TDS the sample is often directly mounted at the manipulator, ensuring ideal thermal and electrical connection to the cryostat manipulator. However, a sample affixed to the manipulator reduces the number of techniques applicable to the sample surface. Here, the setup geometry is usually a limiting factor for multi-tool studies.

In our group structural analysis and spectroscopy on the atomic level is provided by a home-built noncontact atomic force microscopy (nc-AFM) and scanning tunneling microscopy (STM) system.[7–9] For low temperature scanning probe microscopy (SPM) a sample decoupled from the manipulator offers a lot of benefits, in terms of mechanical stability and electrical noise, thermal drift, and cryogenic consumption. Here, a portable sample setup is favored. The integration of TDS in combination with STM has been shown in recent years in the molecular beam and cluster community.[10] To carry out studies with a high-end SPM machine and additional low temperature TDS experiments of a portable sample, we incorporated a specially designed He-flow-through cryostat manipulator into the existing setup.

The sample system chosen for the first measurements with the setup is MgO/Mo(001) and the first probe molecule is CO (mass = 28 amu). CO desorption from MgO surfaces has been studied as a model reaction in heterogeneous catalysis on cleaved MgO(001)[11] and on metal supported MgO-films[12] before but has not been combined with STM experiments so far. The CO desorption of the MgO(001) surface is also used in density functional theory studies as a benchmark system.[6] MgO is used as a support material in heterogeneous catalysis research[13] but also shows direct catalytic properties, e.g., in the oxidative coupling of methane ($2CH_4 + O_2 \longrightarrow C_2H_4 + 2H_2O$),[14] or the water gas shift reaction ($CO + H_2O \rightleftharpoons CO_2 + H_2$).[15] TDS studies of weakly bound gaseous species, e.g., CO or $CH_4$ at oxide surfaces, require minimum sample temperatures as low as 25 K (see Table I). Table I gives the desorption temperature ranges of designated probe molecules for future studies with the described TDS setup from MgO(001).

In this article, we present a versatile setup for low temperature TDS that is introduced into an existing UHV-chamber designed for high resolution SPM measurements at 5 K, including a portable sample setup. The heating is performed via radiative heating from the back side of the sample. A quadrupole mass spectrometer (QMS) equipped with a glass cup, the so-called Feulner cup, is used for detection of the desorbing species.[19] The detailed setup arrangement, its specifications, and the application of the TDS to samples that were also studied with the STM are presented.

## II. EXPERIMENTAL SETUP

### A. Overview

The experimental setup operates under UHV conditions. The base pressure of the UHV-system is $5 \cdot 10^{-10}$ mbar, with a cooled cryostat it attains $1–3 \cdot 10^{-10}$ mbar.

The samples used are metal single crystals with a diameter of 8–11 mm and a thickness of 1–2 mm.

[a]Present address: Institute of Chemistry and Biochemistry, Free University of Berlin, Takustr. 3, 14195 Berlin, Germany.
[b]heyde@fhi-berlin.mpg.de

 © 2016 AIP Publishing LLC
Reuse of AIP Publishing content is subject to the terms at: https://publishing.aip.org/authors/rights-and-permissions. Download to IP: 141.14.132.216 On: Tue, 07 Jun 2016 12:49:53

TABLE I. Desorption peak temperature ranges for desorbing gas from MgO(001) surfaces.

| T (K) | Gas | Substrate | Reference |
|---|---|---|---|
| 25-80 | CO | bulk MgO(001) | Wichtendahl[11] |
| 25-110 | CO | 38 ML MgO/Mo(001) | Dohnálek[12] |
| 30-50 | $CH_4$ | >30 ML MgO/Mo(001) | Tait[16] |
| 120-300 | $CO_2$ | bulk MgO(001) | Chakradhar[17] |
| 130-250 | $D_2O$ | 20 ML MgO/Ag(001) | Włodarczyk[18] |

Sample preparation and analysis are combined in one system. The system consists of a preparation and reaction chamber, as well as a main chamber that houses a dual mode nc-AFM/STM. The microscope is operated at low temperatures (T = 5 K) and works with a portable sample holder system. The detailed microscope setup is described elsewhere.[9]

In Fig. 1 the preparation and reaction chamber of the UHV setup is shown. It is connected to the microscope chamber via a channel that houses the gas-connections for sample preparation. The chamber is also equipped with a sample holder storage unit and with a load-lock for sample transfer to the exterior of the UHV-chamber. The chamber houses standard equipment for surface science sample preparation (sputter gun, heater, evaporators, gas connections) and analysis (low energy electron diffraction, Auger electron spectroscopy), next to a home-built portable quartz micro-balance for evaporator calibration.[20]

The cryostat (in blue) was custom-built and integrated into the manipulator by CryoVac GmbH; it can be cooled with liquid nitrogen or liquid helium. The manipulator is moveable in all three dimensions and fully rotatable around its axis. It offers two mechanical feed-through, one axial for closing and opening the clasp, and one non-axial for the up and down-movement of the exhaust gas-cooled radiation shield. Several electrical connections are integrated: Thermocouple contacts Type K and Type C, one electrical connection to the sample, and connections to the temperature sensing diode in the cryostat and to the internal resistive heater of the cryostat are available. Additionally, gas line in and out connections for the cryogenic fluid are attached on top of the manipulator.

The lower part of the preparation and reaction chamber houses the thermal desorption spectroscopy (TDS) experiment, see dotted circle in Figure 1. An enlarged drawing of the TDS part is displayed in Fig. 2, showing the sample position, as well as the cooling shield location. The sample is in the center of the TDS setup, at the end of the cryostat. A detailed description of the clasp connecting the sample to the cryostat is given in the next section.

A QMS (HAL 201 RC, Hiden Analytical), covered with a custom designed quartz-glass Feulner cup, faces the sample. The sample and a metal ring at the cup's end can be electrically connected for adjustment of the sample-QMS distance via capacitance measurement. The sample is mounted on a sample holder with an opening in the sapphire support behind the sample. This allows direct access of the sample heater to the back side of the crystal. A 50 W tungsten filament of a commercially available halogen lamp (Osram, Halostar

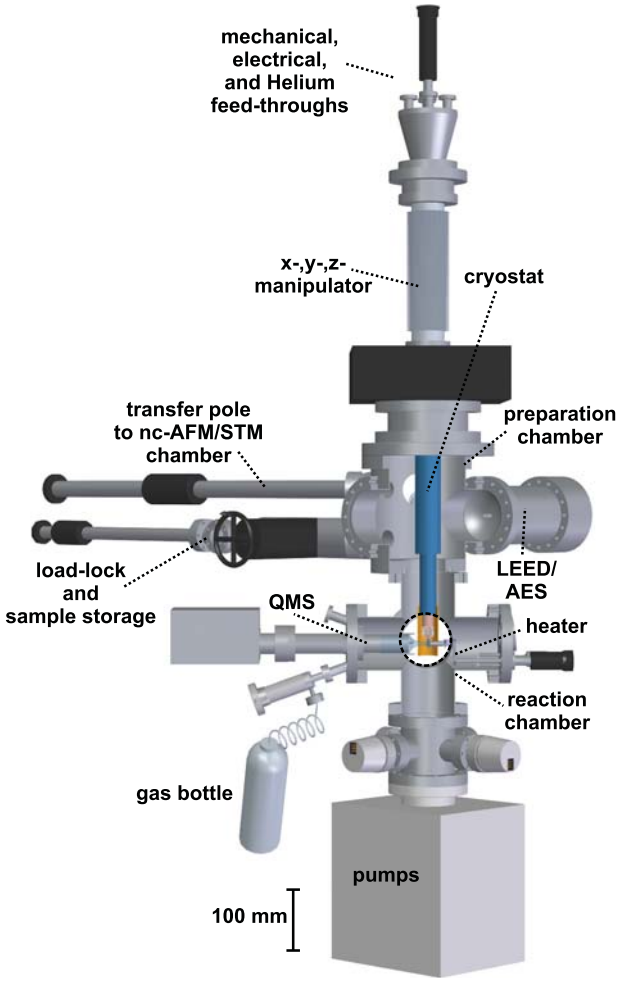


FIG. 1. Drawing of the preparation and reaction UHV-chamber. In the top part is the manipulator with the mechanical, electrical, and helium connections for the sample and the sample cooling. The upper chamber is the preparation chamber, and the lower part houses the reaction chamber which comprises the TDS experiment (encircled).

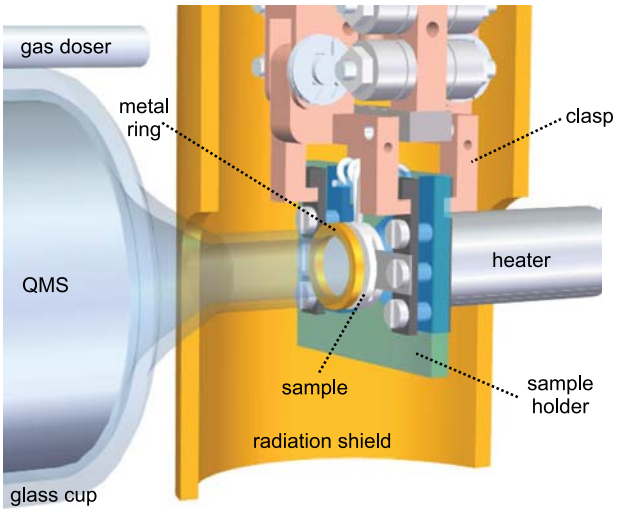


FIG. 2. Schematic showing the sample position in the TDS setup. For a better visibility of the sample, a cut-out of the radiation shield is visualized, showing only the shields back half. In the actual setup the radiation shield fully surrounds the sample.

Reuse of AIP Publishing content is subject to the terms at: https://publishing.aip.org/authors/rights-and-permissions. Download to IP: 141.14.132.216 On: Tue, 07 Jun 2016 12:49:53

64440) is used as a radiative heater from the back side of the sample.[21] For experiments the heater filament distance to the back side of the sample is in the range of 5–10 mm. The sample holder can be covered with an exhaust gas-cooled radiation shield that has openings in the front and in the back for the access of Feulner cup and heater to the sample. In Figure 2 only a cut-out of the radiation shield is visualized, showing the shields back half, for a better visibility of the sample. In the actual setup the radiation shield fully surrounds the sample.

Above the QMS a gas dosing unit is integrated. For gas dosing the sample is positioned in front of the metal tube.

## B. Clasp design

Fig. 3 shows a schematic of the adapter design between cryostat and sample holder, called the clasp. It is a central part of the construction and thus discussed in detail. The electrically insulating parts are colored in light gray (online color: blue); the white colored parts are electrically conductive and not connected to electrical ground; the dark gray colored parts (online color: gray) are electrically conductive and on the same potential as the UHV chamber, on electrical ground.

An axial linear mechanical feed-through (1) is used for opening and closing of the clamping mechanism. A custom built spring mechanism incorporated into the manipulator compensates thermal length variations during cool-down

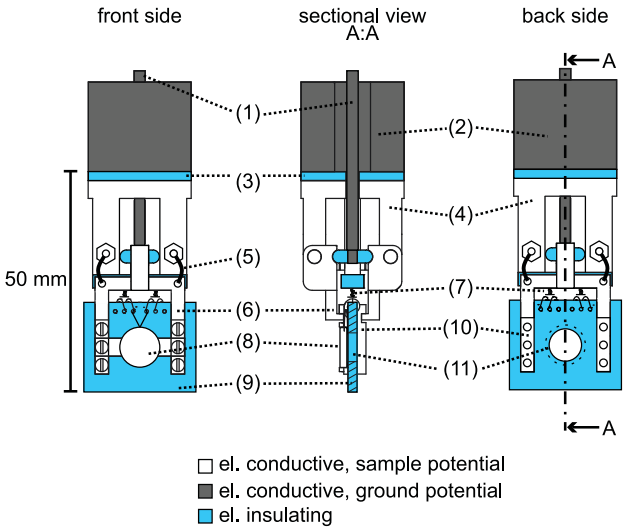


FIG. 3. Schematic drawing of the clasp connecting the sample holder to the cryostat. On the left side is a front view, looking at the surface of the sample. On the right side is a view on the back side of the sample (dashed lines indicate the full sample diameter) and the sample holder, the dashed-dotted line indicates the cut level A of the sectional view shown in the center. (1) axial linear mechanical feed-through for opening and closing of the clasp, (2) cryostat, here T (cryostat) is measured, (3) sapphire disc, (4) copper clasp-base, (5) copper litz wire, thermally connecting the (6) clasp fingers with the clasp-base. The clasp fingers hold the sapphire sample holder via custom designed indented metal bars (10). The copper parts used are gold plated. The thermocouple contact is realized via two separate (7) spring contacts touching the thermocouple wires at the sapphire sample support which are welded to the sample. (8) The sample is fixed with Mo-springs on a (9) sapphire support. The sapphire has a central opening (11) allowing access to the back side of the sample. The legend indicates the color coded electronic properties of the clasp parts.

of the manipulator. This ensures a high pressure of the clasp fingers (6) to the sample holder optimizing the heat transfer.

In the presented setup an adjustable sample potential is needed for sample preparation and analysis. The cryostat (2) is in electrical contact to the chamber; to electrically insulate the sample from the chamber potential a sapphire disc (3) is introduced between cryostat and the copper clasp-base (4). The cryostat temperature is measured with a silicon diode. The clasp base (4) is used for affixing the sample contact wires and thermocouple wires. It also pivots the clasp fingers (6) for movements. Copper litz wires (5) improve the thermal connection between the clasp fingers and the clasp-base. The clasp fingers hold the sapphire sample holder via custom designed indented metal bars (10). The sample (8) is fixed with spring sheets on a sapphire support (9). The sapphire support has a thickness of 2 mm. The thermocouple wires are welded to the sample and fixed at the top of the sapphire support. The sapphire support has a central opening (11) with a diameter of 8.5 mm allowing access to the back side of the sample. The thermocouple contact is realized via two separate (7) spring contacts touching the thermocouple wires at the sapphire sample support that are welded to the sample. An additional non-axial mechanical feed-through for the movement of the radiation shield is not sketched. The radiation shield has openings to allow Feulner-cup and heater access to sample (see Figure 2). The electrically conductive clasp parts, as well as the radiation shield are gold plated to passivate the surfaces regarding chemical reactions.

## C. Cryogenic and electronic circuits

Fig. 4 shows a schematic of the cryogenic (dashed lines) and electronic circuits (solid lines) of the TDS setup.

The cryogenic circuit includes a liquid helium vessel, a transfer tube with a leak-valve connected to the cryostat in

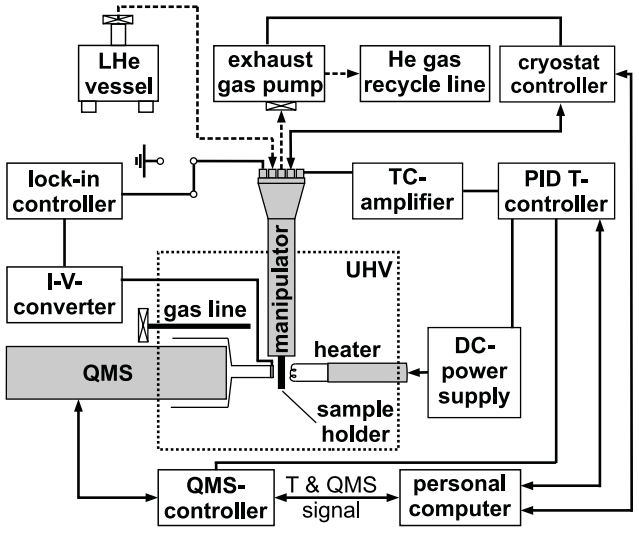


FIG. 4. Diagram of the hardware and the connections of the TDS setup. The gas connections are sketched with dashed lines, the electrical connections with solid lines. Data communication signal lines have arrows at their ends, analog signal lines do not.

Reuse of AIP Publishing content is subject to the terms at: https://publishing.aip.org/authors/rights-and-permissions. Download to IP: 141.14.132.216 On: Tue, 07 Jun 2016 12:49:53

the manipulator, the He-exhaust gas below (heated with an electrical heating hose) connected by means of a magnetic leak valve to a rotary vane pump. The exhaust of the latter is connected to the He-gas-recycle line.

A cryostat controller unit (CTC 100, Stanford Research Systems) controls the helium pump magnet valve, the internal heater of the cryostat and also reads out the Si-Diode cryostat temperature signal.

The sample contact can be used to apply a potential of choice or to electrically ground the sample. To control the sample position, the sample contact and the metal ring at the front of the Feulner cup (details see Fig. 2) are connected to a lock-in controller.

The sample thermocouple (TC) signal is amplified in a TC-amplifier (HS 210-K, Schlichting Physikalische Instrumente) and fed to a proportional–integral–derivative temperature (PID T) control unit (HS 170, Schlichting Physikalische Instrumente). The PID T-controller adjusts the output of the DC-power supply (ES030-5, DeltaElektronika B. V.) to heat the sample. The PID T-control unit is also connected to the personal computer (PC) and forwards an analog signal of the sample temperature to the QMS controller. The QMS-control unit forwards both, the QMS and T-signal simultaneously to the PC.

High voltage (HV) is applicable to the heater filament or to the sample, depending on the experimental requirements. The power supply was customized for HV-based heating by electron bombardment for sample preparation and high temperature-TDS in future experiments.

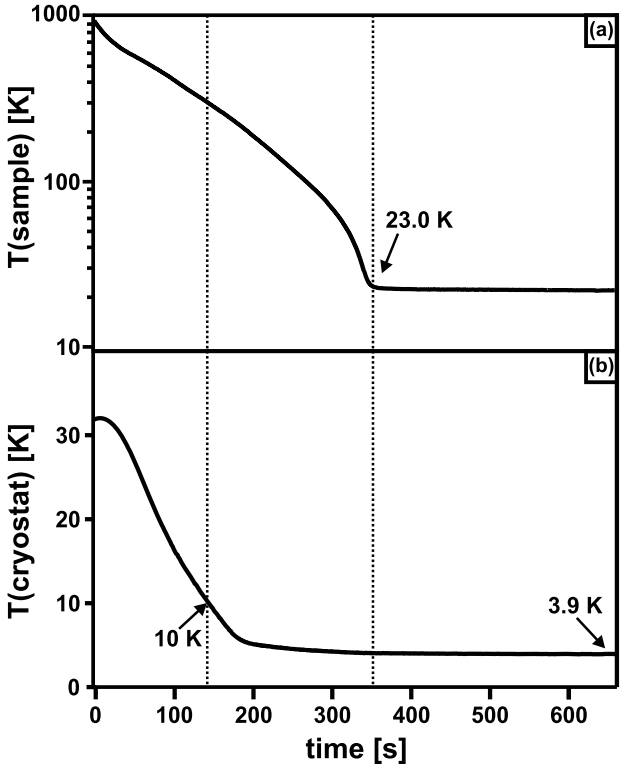


FIG. 5. Cooling performance: temperature of (a) sample, measured with a Type K thermocouple wire and (b) cryostat, measured with a Si-Diode in the cryostat. Cool-down after heating the sample to 940 K. The time scale is set to zero at the beginning of the sample cooling ramp.

## III. PERFORMANCE

### A. Cooling performance

The manipulator setup is designed for sample preparation and for TDS experiments. The maximum temperatures for sample preparation used in the manipulator are annealing steps of 20 min at 1300 K and shorter flashes up to 1530 K.

The cooling is realized via a flow-through-cryostat. The cryostat cooling power (used with liquid helium) is >4 W at 4.2 K, the working temperature lies between 3.5 and 4.2 K, depending on the pressure produced by the exhaust gas pump (see Figure 4). The amount of liquid He needed for the cool-down from room temperature is 2.2 l, while the consumption during a series of measurements lies at 2.4 l/h.

The cooling time for cooling from room temperature to $T_{cryostat}$ = 4.2 K is ~5 min.

From $T_{sample}$ = 150 K to 25 K it takes 132 s (to 22 K it takes 140 s). The cooling performance of the precooled cryostat after heating the sample to 940 K is illustrated in Fig. 5. The top part (a) shows the sample temperature and the bottom part (b) depicts the cryostat temperature. Here, the cryostat maximum temperature is 32 K which is cooled to 10 K in 136 s. By then the sample still has a temperature of 300 K. After 350 s the sample cooling rate drops significantly. The sample is cooled down to 22 K after 600 s.

An important influence on the lowest attainable sample temperature is the effective fixation of the sample on the sample holder. Since the cryostat temperature is considerably lower than the sample temperature, improving the thermal coupling between cryostat and sample will decrease the minimum temperature that can be achieved.

The influence of the radiation shield on the sample temperature is significant, the minimum temperature attained without the radiation shield covering the sample was 30 K. In the here presented experiments the radiation shield covered the sample.

### B. Temperature control

Although resistive heating is the preferred heating method for TDS experiments, the integration was not feasible in the existing setup. Therefore, we work with a radiative heating 50 W filament from the back of the crystal (see Figure 2).

The fastest heating ramp used for TDS measurements with this heater is 2.0 K/s. A linear power ramp with a defined minimum filament current offset is used for heating. The DC power supply is used in voltage control mode with the PID T-controller.

Fig. 6 presents the heating ramp stability during TDS experiments. The heating rate dT/dt is shown as a function of the sample temperature T. The ramp starting temperature $T_0$, as well as $T_{stable}$ from which on the temperature deviation is smaller than 100 mK, is noted in the upper right corner of the figure.

Depending on the heating rate, the temperature ramps reach $T_{stable}$ at 2-10 K above $T_0$. The radiative heater in the setup is able to heat the sample up to 500 K.

Reuse of AIP Publishing content is subject to the terms at: https://publishing.aip.org/authors/rights-and-permissions. Download to IP: 141.14.132.216 On: Tue, 07 Jun 2016 12:49:53

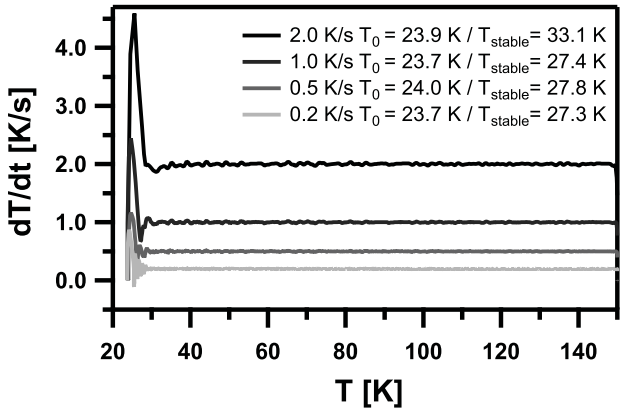


FIG. 6. Illustration of the heating ramp stability during TDS experiments. The heating rate dT/dt is shown as a function of the sample temperature T. The ramp starting temperature $T_0$, as well as $T_{stable}$ after which the temperature deviation is smaller than 100 mK, is noted in the plot's legend.

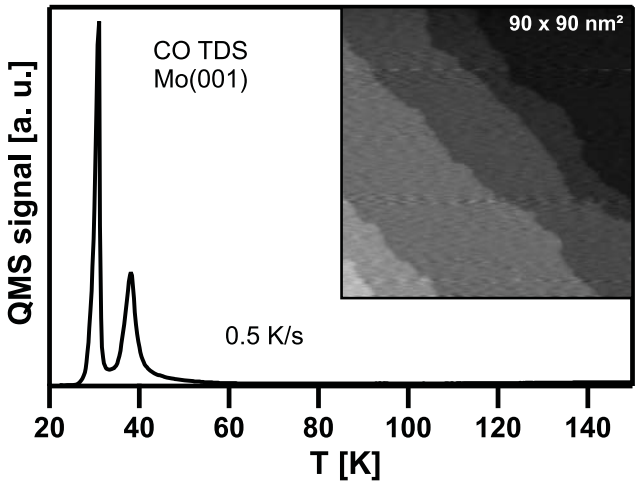


FIG. 7. CO-TDS spectrum of a Mo(001) substrate. The mass spectrometer was set to mass 28 (CO). The initial coverage is 2.7 ML CO. Inset: STM image of Mo(001) recorded with a bias voltage of +1.0 V and a tunneling current setpoint of 50 pA at 5 K. The image size is 90 nm × 90 nm.

### C. Gas dosing and detection

Above the QMS is a metal tube with an opening of 3 mm that is used as the gas doser (see Figure 2). The gas dosing process is executed with a manually operated leak-valve and is monitored with the mass spectrometer signal. The reproducibility of the dosing procedure was verified with a series of experiments. The distance between the doser and the sample can be adjusted from 7 to 32 mm. In the experiments presented here, the dosing unit was located 24 mm in front of the sample surface. The connection to the gas bottle can be filled with gas and goes through a cooling trap filled with liquid nitrogen in the case of the CO experiments.

The QMS is covered with a glass cone, the Feulner cup. The glass cone has an opening with a diameter of 5 mm facing the sample. As developed by Feulner, it is used to increase the signal quality of the experiment.[19] It acts as a gas collector, enhancing the signal of the sample and reducing the background signal. The pressure rise of the desorbing gas from the sample is increased, due to the smaller volume in the cup compared to the whole chamber. Whereas the detection of species desorbing from the surrounding setup parts, such as the sample clasp, the heater, or the radiation shield is minimized.

Additionally, the glass cone is used to measure the desorbing gas of a limited area in the center of the crystal to reduce edge effects (as temperature gradients or inhomogeneous coverage). The cone was manufactured from quartz glass, because of the low reactivity of the material and hence smaller adsorption-desorption disturbances. Drawbacks of the Feulner cup are increasing readsorption, due to the increased pressure in the cup and thus insufficient pumping rates at higher heating ramps.

As shown by Feulner, the distance control between sample and glass cup is crucial for reliable measurements with this setup design. A reproducible distance allows a comparison of absolute signal intensities of measurements. A distance control using capacitive measurements between the sample and a gold plated metal ring is used. It enables a reproduction of the sample-cup-distance with an accuracy in the 10 $\mu$m range. The sample is placed 0.5 mm in front of the glass cup opening for TDS measurements. The base holding the mass spectrometer and the gas collector are designed for possible setup modifications. For example, a gas dosing unit integrated into the gas collector, as used in pulsed temperature programmed reaction measurements,[10] can thus be realized in the future.

To check the CO desorption background signal for further experiments in the range of 25-150 K, thermal desorption spectra of CO desorbing from the bare substrate, a Mo(001) crystal were measured as reference. Since the sample holder is made from sapphire, the spectra were also examined for peaks of CO desorbing from $Al_2O_3$.

The Mo(001) sample was cleaned prior to CO exposure by a series of Ar sputter and UHV-annealing ($T_{max}$ = 1450 K) steps. The CO was dosed at a sample temperature lower than 25 K and the sample heated to 150 K with a constant rate of 0.5 K/s. The resulting desorption spectrum is plotted in Fig. 7. The inset shows an STM image of Mo(001) recorded with a bias voltage of +1.0 V and a tunneling current setpoint of 50 pA. The image size is 90 nm × 90 nm. Terraces and monoatomic steps are visible. A higher resolution reveals small adsorbates on the surface. Auger electron spectroscopy indicates that these features can be assigned to residual C and O impurities.

In the TDS spectrum two desorption peaks are distinguishable. The one at 31.2 K corresponds to CO multilayer desorption and the one at 38.2 K corresponds to desorption of physisorbed CO from the sample, and they are in good agreement with the literature.[22] No other desorption peaks or significant changes of the background are noticeable. The desorption of chemisorbed CO is expected at temperatures above 150 K and not relevant for the background in the presented experiments.[23] A desorption peak at 120 K expected for CO desorbing from sapphire ($Al_2O_3$) is not observed,[24,25] indicating that no significant amount of CO from the sapphire sample support reaches the QMS detector (m/z = 28).

Reuse of AIP Publishing content is subject to the terms at: https://publishing.aip.org/authors/rights-and-permissions. Download to IP: 141.14.132.216 On: Tue, 07 Jun 2016 12:49:53

## IV. APPLICATION TO THE SYSTEM CO ON MGO/MO(001)

The multi-tool setup was applied first to the system CO on MgO/Mo(001). This sample system is employed in heterogeneous catalysis as a model system for desorption processes of oxide materials. Here, we present results of experiments performed on a 10 ML MgO film on a Mo(001) support.

The studied MgO film was prepared in the following way: after cleaning the Mo(001) substrate, as described in Section III C, Mg was evaporated from a carbon crucible onto the surface. During the 10 min deposition (rate = 1 ML/min) the sample was at room temperature and in oxygen atmosphere ($p_{O_2} = 5 \cdot 10^{-7}$ mbar). After deposition, the sample was annealed in UHV for 10 min at 1100 K. Before transfer to the STM and in between TDS measurements the sample was flashed to 900 K to clean the surface from adsorbates. The reproducibility of the TDS was checked via the deposition of equal CO amounts at different stages of the experiment.

The sample preparation was followed by measurements in the STM, see Figs. 8(a) and 8(b). A closed oxide film surface is visible. Line defects, as well as single point defects can be identified. After finishing the experiments in the STM chamber, the sample was transferred to the cryostat-manipulator. Immediately after the sample transfer the cryostat-manipulator was cooled down. For TDS measurements the CO was dosed at a sample temperature lower than 25 K and the sample was linearly heated with a rate of 0.5 K/s. The desorption spectra measured are plotted in Fig. 8(c). Following the TDS measurements, the sample was transferred again to the STM. Figs. 8(d) and 8(e) show STM measurements of the oxide film after the TDS experiments. Here, the oxide film is still closed and exhibits line defects as well as point defects.

The combination of the STM with the TDS experiment allows to detect possible morphological sample changes and the sample stability after the TDS experiments. The sample was characterized with the STM in both cases (pre and post-TDS) at several spots across the sample surface with images on the presented length scale. The STM study of the sample surface before and after CO-TDS experiments reveals no changes of the sample morphology in terms of surface roughness, terrace size, and defect density.

In the TDS spectra two main desorption peaks are distinguishable, see Fig. 8(c). One at 31.6 K labeled with (1), corresponding to multilayer CO desorption, and one at 61.3 K labeled with (2), corresponding to CO desorption from the MgO(001) terrace sites. The desorption features are comparable to studies of Wichtendahl *et al.* on cleaved bulk MgO,[11] and on a Mo(001) supported 38 ML MgO-film.[12] A shallow desorption feature between 65 and 90 K, labeled with (3), can be observed in Fig. 8(c), that is a little bit wider (65–100 K) in the 38 ML film experiment from the literature and not present in the bulk literature desorption spectra. This desorption feature can be assigned to CO desorption from different defect sites present in the film.[12] The spectra differences indicate that the defect level in the presented film is higher than in the cleaved bulk MgO(001) surface and similar to the defect density in the MgO film of Dohnálek *et al.* This defect density differences are supported by a comparison of the STM study of the presented MgO film with nc-AFM data on cleaved MgO(001) surfaces, where the surface morphology mainly consists of large (001) terraces that have a low defect density compared to the thin film systems on Mo(001).[13,26] Differences in the type of defects between the 38 ML MgO film from the literature and the presented system can be explained with differences in the film preparation using 600 K and room temperature during deposition, respectively. As experiments by Gonchar and Risse suggest, the two different ways to grow MgO films on Mo(001) lead to different types of defects being present in the film.[27]

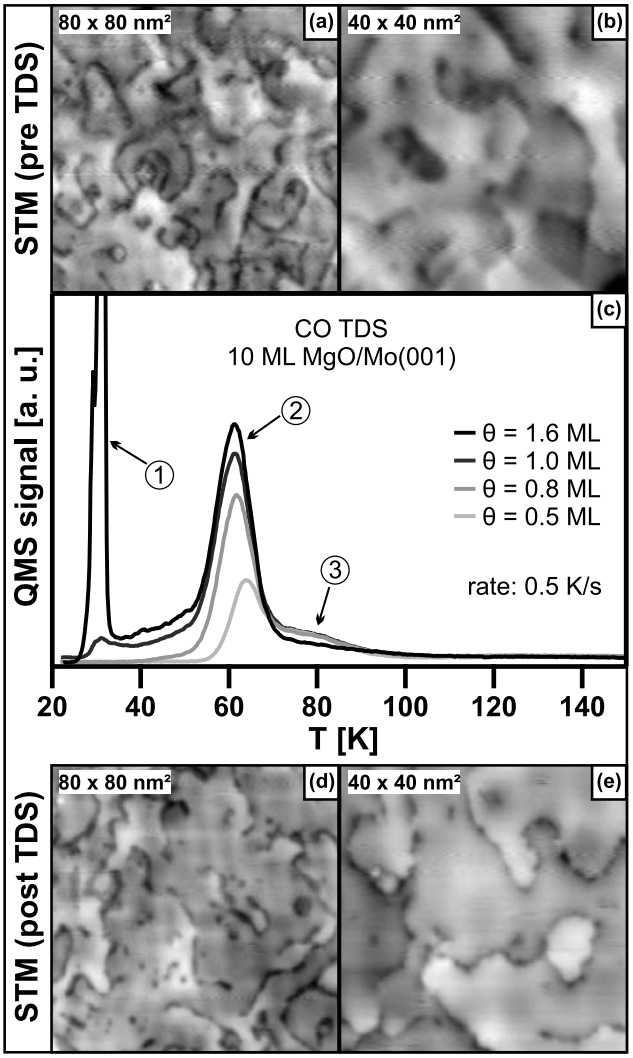


FIG. 8. STM images and CO-TDS spectra of a 10 ML MgO/Mo(001) surface. (a) and (b) show STM images of the 10 ML MgO/Mo(001) recorded before TDS experiments. (c) shows the CO TDS spectra: the initial CO coverages are 0.5, 0.8, 1.0, and 1.6 ML, respectively. The mass spectrometer was set to mass 28 (CO). (d) and (e) show STM images of the 10 ML MgO/Mo(001) recorded after TDS experiments. The STM image sizes are ((a) and (d)) 80 nm × 80 nm and ((b) and (e)) 40 nm × 40 nm. All STM images were recorded with a bias voltage of +5.0 V and a tunneling current setpoint of 10 pA at 5 K.

## V. CONCLUSION

A customizable way of implementing a low temperature TDS experiment to an existing UHV-chamber system working

Reuse of AIP Publishing content is subject to the terms at: https://publishing.aip.org/authors/rights-and-permissions. Download to IP: 141.14.132.216 On: Tue, 07 Jun 2016 12:49:53

with exchangeable samples is introduced. The detailed setup, as well as its application are presented. As a proof of principle, a low temperature TDS study of weakly adsorbing species on a model catalyst is realized. Temperature ramps from below 25 K with a maximum heating rate of 2.0 K/s are feasible. A radiative heater can heat the sample to 500 K. Further developments for a wider range of the experimentally accessible desorption temperatures are in progress. For TDS at higher temperatures a controllable high voltage-power supply is planned for linearly ramped electron bombardment heating to temperatures up to T > 1500 K.

The experiment can be implemented in any existing setup by the introduction of a LHe-cooled flow-through cryostat manipulator with a central mechanical feed-through and a QMS facing a heater on one level for simultaneous gas detection and sample heating. With this device the thermal coupling of the cryostat to the portable sample is realized for cooling to sample temperatures below 25 K.

The sample can be studied before and after TDS with a high-end SPM, allowing spectroscopy at the atomic scale. The combination of low temperature TDS and STM of the same sample is demonstrated on the heterogeneous model catalysis system MgO/Mo(001) with the probe molecule CO. This setup is a further step in the characterization of the same sample with multiple complementary methods. The application is feasible for most portable sample setups, making multi-tool surface science studies and high sample throughput experiments possible.

## ACKNOWLEDGMENTS

The authors gratefully acknowledge the help of Dietrich Menzel and of Jens Hartmann for advice and ideas during the planning phase. We also want to thank Georg Heyne (FHI Elab) and Michael A. Krzyzowski (CryoVac GmbH) for fruitful discussions and technical support. S.S. would like to acknowledge the support from the Deutsche Forschungsgemeinschaft (DFG) through the Cluster of Excellence Unifying Concepts in Catalysis (UNICAT).

[1]G. Ertl and H.-J. Freund, Phys. Today **52**(1), 32 (1999).
[2]P. A. Redhead, Vacuum **12**, 203 (1962).
[3]D. A. King, Surf. Sci. **47**, 384 (1975).
[4]D. Menzel, in *Chemistry and Physics of Solid Surfaces IV*, edited by R. Vanselow and R. Howe (Springer, Berlin, Heidelberg, 1982), Chap. 16, pp. 389–406.
[5]G. Pacchioni, Surf. Rev. Lett. **7**, 277 (2000).
[6]A. D. Boese and J. Sauer, Phys. Chem. Chem. Phys. **15**, 16481 (2013).
[7]M. Heyde, M. Kulawik, H.-P. Rust, and H.-J. Freund, Rev. Sci. Instrum. **75**, 2446 (2004).
[8]H.-P. Rust, M. Heyde, and H.-J. Freund, Rev. Sci. Instrum. **77**, 043710 (2006).
[9]M. Heyde, G. H. Simon, H.-P. Rust, and H.-J. Freund, Appl. Phys. Lett. **89**, 263107 (2006).
[10]S. Bonanni, K. Aït-Mansour, M. Hugentobler, H. Brune, and W. Harbich, Eur. Phys. J. D **63**, 241 (2011).
[11]R. Wichtendahl, M. Rodriguez-Rodrigo, U. Härtel, H. Kuhlenbeck, and H.-J. Freund, Phys. Status Solidi **173**, 93 (1999).
[12]Z. Dohnálek, G. A. Kimmel, S. A. Joyce, P. Ayotte, R. S. Smith, and B. D. Kay, J. Phys. Chem. B **105**, 3747 (2001).
[13]C. Barth and C. R. Henry, J. Phys. Chem. C **113**, 247 (2009).
[14]J. H. Lunsford, Angew. Chem., Int. Ed. Engl. **34**, 970 (1995).
[15]T. Shido, K. Asakura, and Y. Iwasawa, J. Catal. **122**, 55 (1990).
[16]S. L. Tait, Z. Dohnálek, C. T. Campbell, and B. D. Kay, J. Chem. Phys. **122**, 164708 (2005).
[17]A. Chakradhar and U. Burghaus, Surf. Sci. **616**, 171 (2013).
[18]R. Włodarczyk, M. Sierka, K. Kwapien, J. Sauer, E. Carrasco, A. Aumer, J. F. Gomes, M. Sterrer, and H.-J. Freund, J. Phys. Chem. C **115**, 6764 (2011).
[19]P. Feulner, J. Vac. Sci. Technol. **17**, 662 (1980).
[20]S. Stuckenholz, C. Büchner, G. Thielsch, M. Heyde, and H.-J. Freund, Rev. Sci. Instrum. **84**, 085118 (2013).
[21]J. T. Yates, Jr., *Experimental Innovations in Surface Science: A Guide to Practical Laboratory Methods and Instruments* (AIP Press, 1998).
[22]H. Schlichting and D. Menzel, Rev. Sci. Instrum. **64**, 2013 (1993).
[23]N. V. Petrova, V. D. Osovskii, D. Yu. Balakin, I. N. Yakovkin, and Yu. G. Ptushinskii, Ukr. J. Phys. **56**(3), 272 (2011).
[24]G. S. Hsiao, W. Erley, and H. Ibach, Surf. Sci. **405**, L465 (1998).
[25]S. Raaen and X. Yu, Appl. Surf. Sci. **349**, 17 (2015).
[26]T. V. Ashworth, C. L. Pang, P. L. Wincott, D. J. Vaughan, and G. Thornton, Appl. Surf. Sci. **210**, 2 (2003).
[27]A. Gonchar and T. Risse, Mol. Phys. **111**, 2708 (2013).

Reuse of AIP Publishing content is subject to the terms at: https://publishing.aip.org/authors/rights-and-permissions. Download to IP: 141.14.132.216 On: Tue, 07 Jun 2016 12:49:53